Journal of Innovative Optical Health Sciences
Vol. 12, No. 1 (2019) 1841003 (7 pages)

DOI: 10.1142/S1793545818410031

World Scientific
www.worldscientific.com

High-resolution imaging of graphene by tip-enhanced coherent anti-Stokes Raman scattering

Xiaolong Kou, Qian Zhou, Dong Wang, Jinghe Yuan*,
Xiaohong Fang† and Lijun Wan
CAS Key Laboratory of Molecular Nanostructure and Nanotechnology
Institute of Chemistry Chinese Academy of Science
Beijing 100190, P. R. China
**jhyuan@iccas.ac.cn*
†*xfang@iccas.ac.cn*

Received 28 October 2018
Accepted 10 December 2018
Published 23 January 2019

Coherent anti-Stokes Raman scattering (CARS) is able to enhance molecular signals by vibrational coherence compared to weak Raman signal. The surface or tip enhancement are successful technologies, which make it possible for Raman to detect single molecule with nanometer resolution. However, due to technical difficulties, tip-enhanced CARS (TECARS) is not as successful as expected. For single molecular detection, high sensitivity and resolution are two main challenges. Here, we reported the first single atom layer TECARS imaging on Graphene with the highest resolution about 20 nm, which has ever been reported. The highest $EF_{TECARS/CARS}$ is about 10^4, the similar order of magnitude with SECARS (EF of tip is usually smaller than that of substrates). Such resolution and sensitivity is promising for medical, biology and chemical applications in the future.

Keywords: Tip-enhanced coherent anti-Stokes Raman scattering; CARS; graphene.

1. Introduction

Raman spectroscopy provides molecular vibrational fingerprint information and has been widely used in medicine, biology, materialogy, chemical engineering and bromatology. Compared to weak spontaneous Raman signal, coherent anti-Stokes Raman scattering (CARS) can enhance molecular signals by vibrational coherence.[1,2] CARS is a third-order nonlinear Raman imaging modality,[3] which needs three incident fields including a pump flied (ω_1), a Stokes flied (ω_2; $\omega_2 < \omega_1$), and a probe flied (ω_1). With a high numerical aperture (NA) objective lens, the phase matching condition can be satisfied at the focused light spot.[4,5] The anti-Stokes signal ($2\omega_1 - \omega_2$) will be generated if the difference frequency of flied pump and Stokes ($\omega_1 - \omega_2$) coincides with molecular vibrational frequency (Fig. 1).

*,†Corresponding authors.

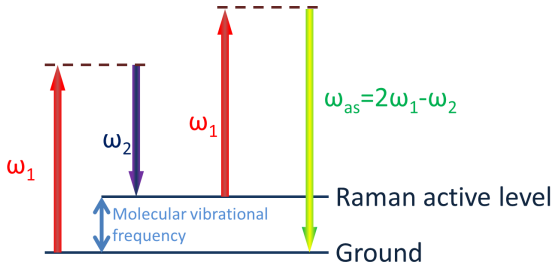

Fig. 1. Energy diagram of CARS process.

CARS microscopy can achieve submicron scale three-dimensional imaging.[6,7] However, the resolution is still limited by the light diffraction (which is about 300 nm).[6] To achieve both higher resolution and signal sensitivity, several novel methods have been proposed such as structured illumination in wide-field CARS microscopy,[8–10] fiber probe tip near-field scanning,[11] and also electric field enhancement effect[12] including surface enhancements[13–17] and tip enhancements.[18]

The field enhancement effect is attributed to the excitation of the local mode of the surface plasmon polaritons,[12] and was wildly applied to the amplification of light emission such as: two-photon-excited fluorescence,[19] infrared absorption,[20,21] fluorescence,[22] and Raman spectroscopy. In Raman, this technique is well known as surface enhanced Raman scattering (SERS)[23–25] and tip enhanced Raman scattering (TERS).[26–28]

In the past decade, TERS becomes a promising technique. With a "hot" tip apex, it is possible to detect the Raman signal from a single molecule, and even from a single chemical bond[29,30] with spatial resolution down to 1 nm.[31,32]

However, due to technical challenges, the surface enhanced CARS (SECARS) and tip enhanced CARS (TECARS) didn't show a higher sensitivity and resolution as expected, and the enhancement effect is one of the challenges: The SECARS enhancement factor (EF) over CARS ($EF_{SECARS/CARS}$) can theoretically reach 10^8–10^{24} and $EF_{SECARS/Raman}$ can even reach 10^{14}–10^{30},[33] which has not yet been experimentally demonstrated. In general, the near-field enhancement of tip is smaller than that of substrates, and because of which, the $EF_{TECARS/CARS}$ has not even been measured in the recent reports of TECARS.[17,18,34,35]

Due to technical difficulties, the reported spatial resolution in TECARS microscopy is far less than expected (20 nm for DNA cluster[18]; ~80 nm for cell membrane[34] and ~60 nm for carbon nanotube clusters[17,35]). The single molecule detection by TECARS has never been achieved yet.

In this paper, graphene sample was imaged by TECARS, and this is the first TECARS report imaging single atom layer at one of the highest resolutions of 20 nm by Au tip. The highest $EF_{TECARS/CARS}$ is about 10^4, which is even close to SECARS[36,37] and had never been seen in TECARS experiments before. With technological improvement, it is expected that there is a bright future for biological, chemical and medical application of TECARS.

2. Methods and Materials

2.1. *TECARS system and measurement*

The TECARS microscopy system is shown in Fig. 2, which is a combination of a homemade CARS microscope and an atomic-force microscope (AFM).

The homemade CARS microscope is equipped with two mode-locked Ti:sapphire lasers pulse (Coherent Inc., Mira HP-F laser, pulse duration 2 ps, pulse repetition rate 76 MHz), and an inverted optical microscope (Nanofinder HE, Tokyo Instruments, Inc.) with the built-in 532 nm Raman laser, an EMCCD (Newton DU920P-BEX2-DD), an avalanche photodiode (APD, Martock Design Ltd) and AFM (AIST-NT, Combiscop^{TM}-1000 SPM).

ω_1 and ω_2 beams are collinearly overlapped in time and space ($\omega_1 = 861$ nm and $\omega_2 = 756$ nm), and introduced into the microscope system with an objective lens (immersion: air, magnification: 60×, Numerical aperture: 0.9, RMS60X-PFC, Olympus) focused onto the sample surface. The optical pulses synchronization was controlled by synchro-lock advanced performance system (Synchro-Lock AP controller, Coherent Inc.). The AFM controlled probe tip contacts the sample surface with the constant force and is illuminated by the focused spot. The repetition rate of the excitation lasers is controlled by a pulse picker (Conoptics Model 25D). CARS emission is collected with the same objective lens and detected with the APD. During measurement, the repetition rate was reduced to about 25 MHz and the average power is about 1 mW. The exposure time of each pixel is 50 ms.

Raman spectrum was excited by the built-in 532 nm Raman laser at about 1 mW. 60 × objective lens (immersion: air, Numerical aperture: 0.9,

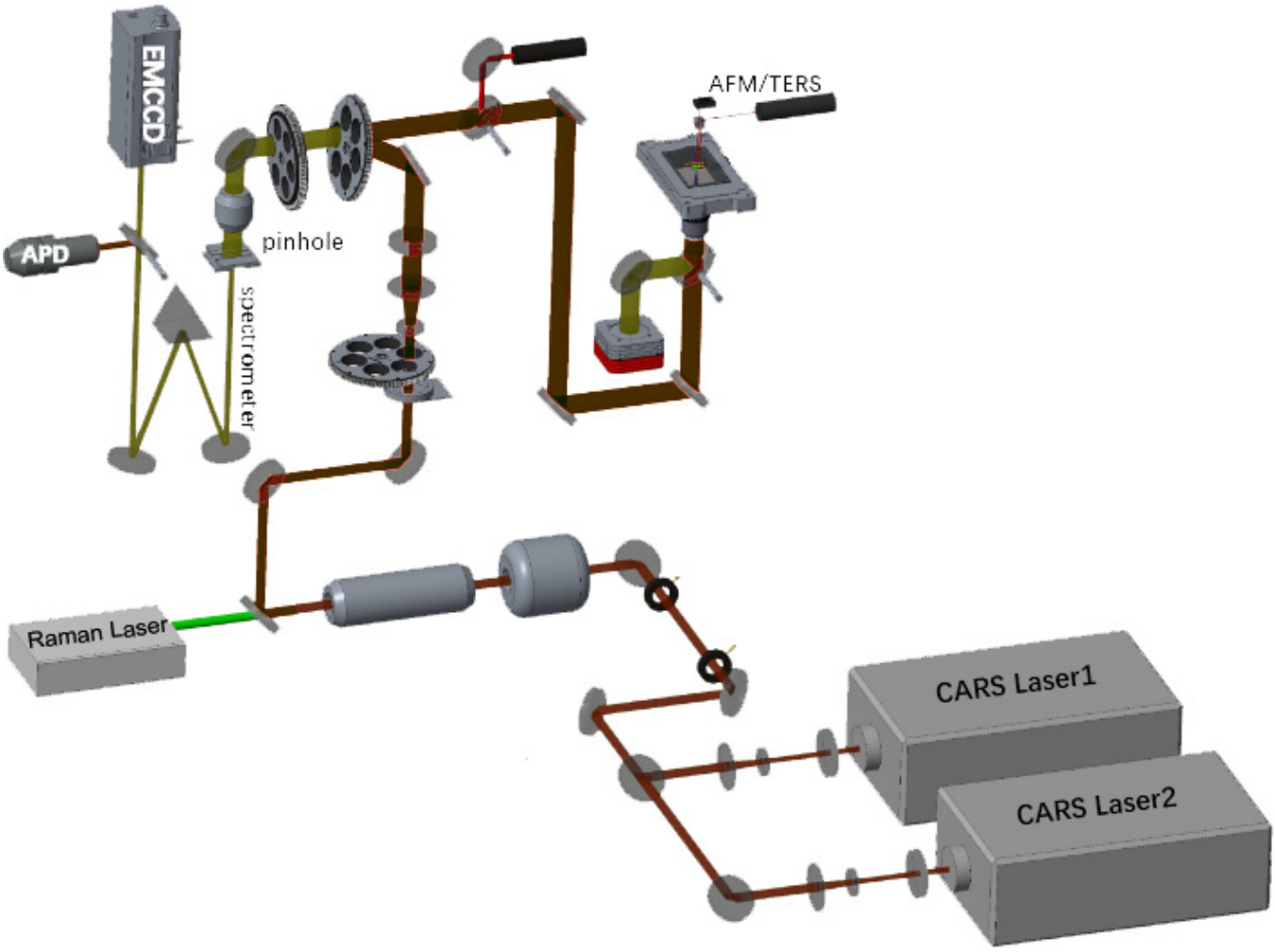

Fig. 2. Schematic of TECARS microscope.

RMS60X-PFC, Olympus) was used for both exciting and detection. CCD detector was calibrated by the built in calibration laser.

2.2. *Tip and sample preparation*

AFM tip was purchased from Nanosensors (ATEC-NC-50), and metal coating of the 20 nm Au was carried out by E-beam evaporation (Edwards, BOC-500).

Graphene was grown through chemical vapor deposition (CVD) method, as reported previously,[38] and in brief: 10% HCl cleaned Cu foil was inserted into the corundum tube inside a horizontal furnace and heated in H_2/Ar at 1000°C. Graphene nuclei was formed with 0.05% methane in Ar for 10 min. Then the flow rate of Ar is increased for 15 min in order to enlarge the graphene nuclei size. After growth, the furnace cooled down quickly.

Then, graphene was transferred onto glass substrate by wet-transfer method[39]: In general, one side of the graphene/Cu foil was spin-coated with (Poly (methyl methacrylate) (PMMA), (950 PMMA, MicroChem) and heated at 120°C for 1 min. The other side of the graphene was removed by O-plasma. Cu foil was etched overnight by 0.1 M $(NH_4)_2S_2O_8$ (Sigma Aldrich). After cleaning by deionized water, the graphene/PMMA film was picked up by glass substrate, and dried in vacuum. Finally, hot acetone was sued to dissolve PMMA for 1 h.

3. Results and Discussion

3.1. *Graph imaging*

One of the main challenges of TECARS is the single molecular detection, which has never been reported before. Here, graphene is chosen for TECARS measurement. As a two-dimensional building block

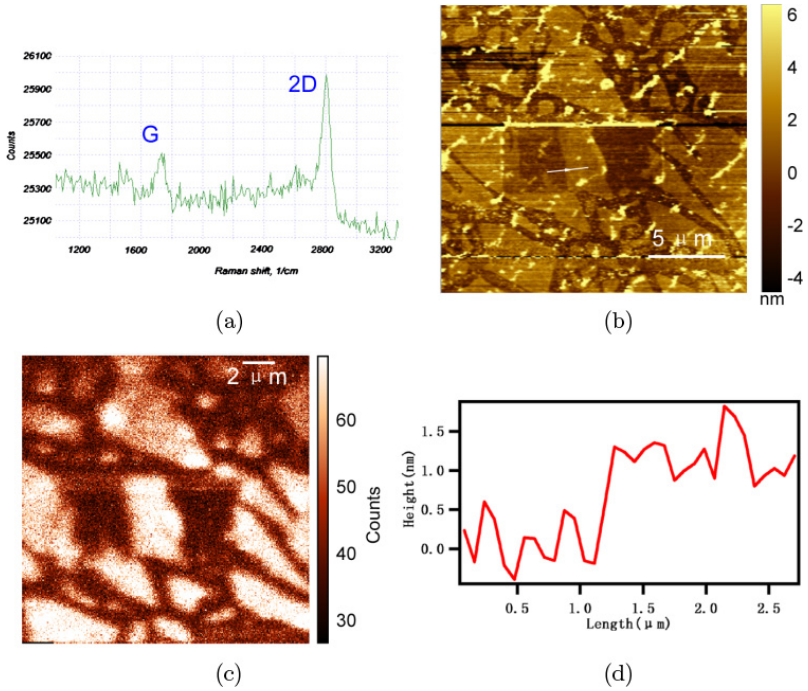

Fig. 3. (a) Raman spectrum of graphene. (b) CARS, (c) AFM image and (d) height measurement of graphene layer by AFM.

of carbon allotropes, graphene plays an important role since its electronic properties.[40–44] The Raman spectra of graphene sheet is shown in Fig. 3(a), the 2D band is characterized by a single peak and the intensity is about 4 times stronger than the G peak, which indicated that the graphene sample is a single layer graphene.[45]

The AFM imaging are shown in Fig. 3(c). The height of graphene is about 1 nm (Fig. 3(d)), which again demonstrated the single graphene layer.

TECARS measurements of graphene G band were carried out. The coherent anti-Stokes signal of G band (at $1612\,\mathrm{cm}^{-1}$) was excited by 861 nm (Stokes) and 756 (pump and probe), and the CARS signal was detected at 674 nm by APD (Figs. 3(b) and 4). The 20 nm gold covered tip was used for signal enhancement.

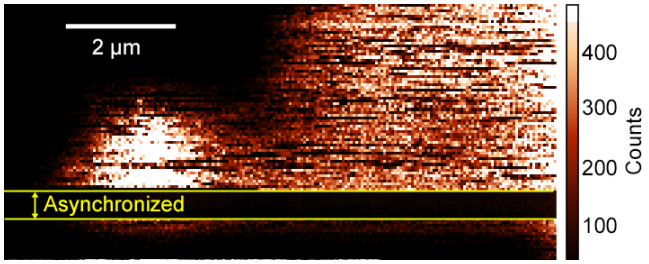

Fig. 4. CARS image with synchronized pulses and asynchronized pulses (yellow part).

CARS process is a third-order nonlinear scattering, which need the spatial overlap and time synchronization of pump, probe and Stokes pulses. Figure 4 shows the CARS signal was generated only when the tow incident laser pulses are synchronized, which suggested the signal was generated by vibrational coherence.

3.2. *The enhancement factor*

Another technical difficulty of enhanced CARS is that the EF is always not as high as expected. Surface EF over CARS are denoted as $\mathrm{EF}_{\mathrm{SECARS/CARS}} \propto |g_p|^4|g_S|^2|g_{\mathrm{aS}}|^2$, where g_p, g_S and g_{aS} are the near-field EFs of the pump, Stokes and anti-Stokes signal, which can theoretically reach 10^8–10^{24}, and $\mathrm{EF}_{\mathrm{SECARS/Raman}}$ can reach 10^{14}–10^{30} in Ref. 33, but never been reached in experiments. The near-field EF of tip is smaller than that of substrates, it is expected that the $\mathrm{EF}_{\mathrm{TECARS/CARS}}$ should be lower than SECARS and may be hard to measure, and the reported TECARS experiments has never shown the EF. Here, we experimentally found the highest $\mathrm{EF}_{\mathrm{TECARS/CARS}}$ can reach 10^4 which is even almost near the EF of SECARS.[36,37] Figure 5 shows the TECARS imaging of graphene with tip approaching the sample (Figs. 5(a) and 5(b)). Compared to control experiment (tip only, without graphene. Figures 5(c) and 5(d)), the

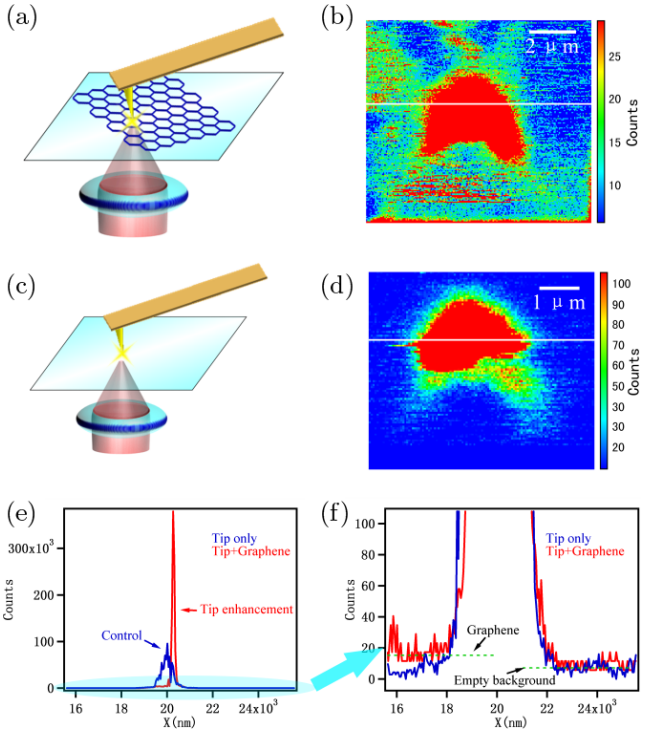

Fig. 5. The measurement of tip enhancement effect. (a) and (b) The CARS imaging of both graphene and Au coated tip. (c) and (d) The control group in which only tip was imaged by CARS. (e) and (f) The signal intensity measurement of the white line in (b) (red) and (d) (blue).

TECARS signal intensity of graphene and background signal near the tip apex are about 3.8×10^5 and 9.6×10^4 Counts, respectively (Fig. 5(e)). With the background subtracted, the intensity is about 2.9×10^5 Counts ($3.8 \times 10^5 - 9.6 \times 10^4$). The signal intensity without enhancement effect can be obtained in the region distant from tip which are about 18 and 8 Counts corresponding to the Graphene and background, respectively (Fig. 5(f)), and after deducting the background, the CARS signal intensity is 10 Counts. The $\mathrm{EF}_{\mathrm{TECARS/CARS}}$ is about 3×10^4, close to SECARS EF,[36,37] calculated by the equation $\mathrm{EF} = \frac{I_{\mathrm{nf}}/N_{\mathrm{nf}}}{I_{\mathrm{ff}}/N_{\mathrm{ff}}}$, where I_{nf} and I_{ff} are the near-field and far-field intensities and N_{nf} and N_{ff} are the corresponding numbers of molecules contributing to each signal.[46]

3.3. *Spatial resolution*

One of the most important technical challenges in TECARS, which attracts the most attention, is spatial resolution. To evaluate the resolution, a smaller scanning step as 10 nm was set. The spatial resolution can be computed as the lateral distance between 20% and 80% of the edge's height.[47] Figure 6 shows the highest resolution is about 20 nm, which is the same as the highest resolution of TECARS imaging which has ever been reported (with DNA sample clusters).[18]

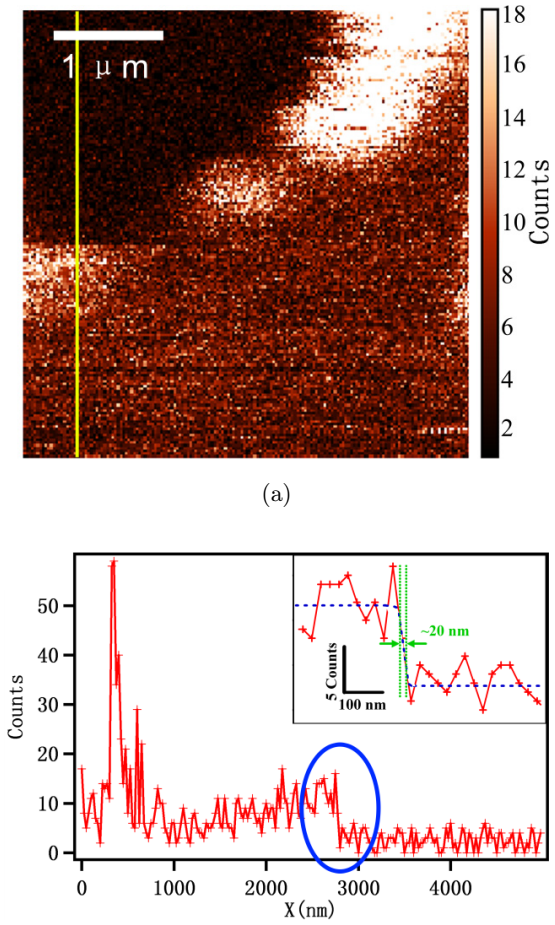

Fig. 6. (a) TECARS imaging of graphene. (b) Signal intensity measurement of the yellow line in (a).

4. Conclusion

In conclusion, here we first reported the single atom layer TECARS imaging, since the single layer graphene can be characterized by both AFM imaging and Raman spectra. Before this, single molecular detection by TECARS has only been theoretically demonstrated. Sensitivity, EF and resolution are the major challenges of TECARS technique and our data show the highest $\mathrm{EF}_{\mathrm{TECARS/CARS}}$ is about $\sim 10^4$, which has never been measured in TECARS reports and have the similar order of magnitude

with SECARS[36,37] (EF of tip is usually smaller than that of substrates). The highest resolution is about 20 nm, the same as the highest TECARS resolution which have ever been reported.[18]

TECARS imaging can be a promising tool for studying morphological, biochemical of materials and live cells at the molecular and subcellular levels without labeling. It is anticipated that imaging quality can be improved significantly by optimizing the tip, polarization laser pulse shaping and also optical path optimization to perform more accurate TECARS imaging in the future.

Conflict of Interest

The authors declare no competing financial interest.

Acknowledgments

We gratefully acknowledge the support from the National Natural Science Foundation of China (Nos. 21735006 and 21127901), and the CAS Key Technology Talent Program.

References

1. R. W. Minck, R. W. Terhune, W. G. Rado, "Laser-stimulated Raman effect and tesonant four-photon interactions in gases H2, D2, and CH4," *Appl. Phys. Lett.* **3**, 181–184 (1963).
2. G. L. Eesley, "Coherent Raman-spectroscopy," *J. Quant. Spectrosc. Radiat.* **22**, 507–576 (1979).
3. M. Levenson, *The Principles of Nonlinear Optics*, Wiley, New York (1984).
4. M. Hashimoto, T. Araki, "Three-dimensional transfer functions of coherent anti-Stokes Raman scattering microscopy," *J. Opt. Soc. Am. A* **18**, 771 (2001).
5. J. X. Cheng, A. Volkmer, X. S. Xie, "Theoretical and experimental characterization of coherent anti-Stokes Raman scattering microscopy," *J. Opt. Soc. Am. B* **19**, 1363–1375 (2002).
6. A. Zumbusch, G. R. Holtom, X. S. Xie, "Three-dimensional vibrational imaging by coherent anti-stokes Raman scattering," *Phys. Rev. Lett.* **82**, 4142–4145 (1999).
7. M. Hashimoto, T. Araki, S. Kawata, "Molecular vibration imaging in the fingerprint region by use of coherent anti-Stokes Raman scattering microscopy with a collinear configuration," *Opt. Lett.* **25**, 1768–1770 (2000).
8. C. Cleff, C. Fallnich, C. J. Lee, H. L. Offerhaus, J. L. Herek, K. J. Boller, P. Groß, W. P. Beeker, "A route to sub-diffraction-limited CARS microscopy," *Opt. Exp.* **17**, 22632–22638 (2009).
9. W. Liu, H. Niu, "Diffraction barrier breakthrough in coherent anti-Stokes Raman scattering microscopy by additional probe-beam-induced phonon depletion," *Phys. Rev. A* **83**, 4795–4804 (2011).
10. S. W. Hell, J. Wichmann, "Breaking the diffraction resolution limit by stimulated emission: Stimulated-emission-depletion fluorescence microscopy," *Opt. Lett.* **19**, 780–782 (1994).
11. R. D. Schaller, J. Ziegelbauer, L. F. Lee, L. H. Haber, R. J. Saykally, "Chemically selective imaging of subcellular structure in human hepatocytes with coherent anti-Stokes Raman scattering (CARS) near-field scanning optical microscopy (NSOM)," *J. Phys. Chem. B* **106**, 8489–8492 (2002).
12. S. Kawata, *Near-field Optics and Surface Plasmon Polaritons*, Springer, Berlin (2001).
13. E. J. Liang, A. Weippert, J. M. Funk, A. Materny, W. Kiefer, "Experimental observation of surface-enhanced coherent anti-Stokes Raman scattering," *Chem. Phys. Lett.* **227**, 115–120 (1994).
14. T. W. Koo, S. Chan, A. A. Berlin, "Single-molecule detection of biomolecules by surface-enhanced coherent anti-Stokes Raman scattering," *Opt. Lett.* **30**, 1024–1026 (2005).
15. C. J. Addison, S. O. Konorov, A. G. Brolo, M. W. Blades, R. F. B. Turner, "Tuning gold nanoparticle self-assembly for optimum coherent anti-stokes Raman scattering and second harmonic generation response," *J. Phys. Chem. C* **113**, 3586–3592 (2009).
16. V. Namboodiri, M. Namboodiri, G. I. C. Diaz, M. Oppermann, G. Flachenecker, A. Materny, "Surface-enhanced femtosecond CARS spectroscopy (SE-CARS) on pyridine," *Vib. Spectrosc.* **56**, 9–12 (2011).
17. N. Hayazawa, T. Ichimura, M. Hashimoto, Y. Inouye, S. Kawata, "Amplification of coherent anti-Stokes Raman scattering by a metallic nanostructure for a high resolution vibration microscopy," *J. Appl. Phys.* **95**, 2676–2681 (2004).
18. T. Ichimura, N. Hayazawa, M. Hashimoto, Y. Inouye, S. Kawata, "Tip-enhanced coherent anti-stokes Raman scattering for vibrational nanoimaging," *Phys. Rev. Lett.* **92**, 220801 (2004).
19. E. J. Sánchez, L. Novotny, X. S. Xie, "Near-field fluorescence microscopy based on two-photon excitation with metal tips," *Phys. Rev. Lett.* **82**, 4014–4017 (1999).
20. A. Lahrech, R. Bachelot, P. Gleyzes, A. C. Boccara, "Infrared-reflection-mode near-field microscopy using an apertureless probe with a resolution of lambda/600," *Opt. Lett.* **21**, 1315–1317 (1996).
21. B. Knoll, F. Keilmann, "Near-field probing of vibrational absorption for chemical microscopy," *Nature* **399**, 134–137 (1999).

22. H. F. Hamann, A. Gallagher, D. J. Nesbitt, "Near-field fluorescence imaging by localized field enhancement near a sharp probe tip," *Appl. Phys. Lett.* **76**, 1953–1955 (2000).
23. M. Fleischmann, P. J. Hendra, A. J. Mcquillan, "Raman spectra of pyridine adsorbed at a silver electrode," *Chem. Phys. Lett.* **26**, 163–166 (1974).
24. D. L. Jeanmaire, R. P. V. Duyne, "Surface Raman spectroelectrochemistry: Part I. Heterocyclic, aromatic, and aliphatic amines adsorbed on the anodized silver electrode," *J. Electroanal. Chem.* **84**, 1–20 (1977).
25. M. G. Albrecht, J. A. Creighton, "Anomalously intense Raman spectra of pyridine at a silver electrode," *Chem. Inform.* **8**, 5215–5217 (1977).
26. R. M. Stöckle, Y. D. Suh, V. Deckert, R. Zenobi, "Nanoscale chemical analysis by tip-enhanced Raman spectroscopy," *Chem. Phys. Lett.* **318**, 131–136 (2000).
27. M. S. Anderson, "Locally enhanced Raman spectroscopy with an atomic force microscope," *Appl. Phys. Lett.* **76**, 3130–3132 (2000).
28. N. Hayazawa, Y. Inouye, Z. Sekkat, S. Kawata, "Metallized tip amplification of near-field Raman scattering," *Opt. Commun.* **183**, 333–336 (2000).
29. C. C. Neacsu, J. Dreyer, N. Behr, M. B. Raschke, "Scanning-probe Raman spectroscopy with single-molecule sensitivity," *Phys. Rev. B* **73**, 193406 (2006).
30. J. Steidtner, B. Pettinger, "Tip-enhanced Raman spectroscopy and microscopy on single dye molecules with 15 nm resolution," *Phys. Rev. Lett.* **100**, 236101 (2008).
31. S. Jiang, Y. Zhang, R. Zhang, C. Hu, M. Liao, Y. Luo, J. Yang, Z. Dong, J. G. Hou, "Distinguishing adjacent molecules on a surface using plasmon-enhanced Raman scattering," *Nat. Nanotechnol.* **10**, 865–869 (2015).
32. R. Zhang, Y. Zhang, Z. C. Dong, S. Jiang, C. Zhang, L. G. Chen, L. Zhang, Y. Liao, J. Aizpurua, Y. Luo, "Chemical mapping of a single molecule by plasmon-enhanced Raman scattering," *Nature* **498**, 82–86 (2013).
33. D. V. Voronine, Z. Zhang, A. V. Sokolov, M. O. Scully, "Surface-enhanced FAST CARS: En route to quantum nano-biophotonics," *Nanophotonics* **7**, 523–548 (2018).
34. J. Lin, K. Z. Jian Er, W. Zheng, Z. Huang, "Radially polarized tip-enhanced near-field coherent anti-Stokes Raman scattering microscopy for bioimaging," *Appl. Phys. Lett.* **103**, 4142–4145 (2012).
35. K. Furusawa, N. Hayazawa, F. C. Catalan, T. Okamoto, S. Kawata, "Tip-enhanced broadband CARS spectroscopy and imaging using a photonic crystal fiber based broadband light source," *J. Raman Spectrosc.* **43**, 656–661 (2012).
36. C. Steuwe, C. F. Kaminski, J. J. Baumberg, S. Mahajan, "Surface enhanced coherent anti-Stokes Raman scattering on nanostructured gold surfaces," *Nano Lett.* **11**, 5339 (2011).
37. M. Yan, L. Zhang, Q. Hao, X. Shen, X. Qian, H. Chen, X. Ren, H. Zeng, "Surface-enhanced dual-comb coherent Raman spectroscopy with nanoporous gold films," *Laser. Photonics Rev.* **12**, 1800096 (2018).
38. J. Li, H. Ji, X. Zhang, X. Wang, Z. Jin, D. Wang, L. J. Wan, "Controllable atmospheric pressure growth of mono-layer, bi-layer and tri-layer graphene," *Chem. Commun.* **50**, 11012–11015 (2014).
39. I. N. Kholmanov, C. W. Magnuson, A. E. Aliev, H. Li, B. Zhang, J. W. Suk, L. L. Zhang, E. Peng, S. H. Mousavi, A. B. Khanikaev, "Improved electrical conductivity of graphene films integrated with metal nanowires," *Nano Lett.* **12**, 5679 (2012).
40. K. S. Novoselov, E. Mccann, S. V. Morozov, V. I. Falko, M. I. Katsnelson, U. Zeitler, D. Jiang, F. Schedin, A. K. Geim, "Unconventional quantum Hall effect and Berry's phase of 2 in bilayer graphene," *Nat. Phys.* **2**, 177–180 (2006).
41. K. S. Novoselov, D. Jiang, F. Schedin, T. J. Booth, V. V. Khotkevich, S. V. Morozov, A. K. Geim, "Two-dimensional atomic crystals," *Proc. Natl. Acad. Sci. USA* **102**, 10451–10453 (2005).
42. K. S. Novoselov, A. K. Geim, S. V. Morozov, D. Jiang, M. I. Katsnelson, I. V. Grigorieva, S. V. Dubonos, A. A. Firsov, "Two-dimensional gas of massless Dirac fermions in graphene," *Nature* **438**, 197–200 (2005).
43. Y. Zhang, Y. W. Tan, H. L. Stormer, P. Kim, "Experimental observation of the quantum Hall effect and Berry's phase in graphene," *Nature* **438**, 201–204 (2005).
44. K. S. Novoselov, A. K. Geim, S. V. Morozov, D. Jiang, Y. Zhang, S. V. Dubonos, I. V. Grigorieva, A. A. Firsov, "Electric field effect in atomically thin Carbon films," *Science* **306**, 666–669 (2004).
45. A. C. Ferrari, J. C. Meyer, V. Scardaci, C. Casiraghi, M. Lazzeri, F. Mauri, S. Piscanec, D. Jiang, K. S. Novoselov, S. Roth, "Raman spectrum of graphene and graphene layers," *Phys. Rev. Lett.* **97**, 187401 (2006).
46. B. Pettinger, G. Picardi, R. Schuster, G. Ertl, "Surface-enhanced and STM tip-enhanced Raman spectroscopy of CN – ions at gold surfaces," *J. Electroanal. Chem.* **554**, 293–299 (2003).
47. F. Kollmer, W. Paul, M. Krehl, E. Niehuis, "Ultra high spatial resolution SIMS with cluster ions - approaching the physical limits," *Surf. Interface Anal.* **45**, 312–314 (2013).